Experimental investigation of an accidental ice impact on an aluminium high speed craft

H. Herrnring, J.M. Kubiczek & S. Ehlers
Hamburg University of Technology, Hamburg, Germany

N.O. Niclasen & M. Burmann
KTH Royal Institute of Technology, Stockholm, Sweden

ABSTRACT: High speed vessels are constructed according to the high speed craft codes. These codes enable very light ship structures, which are necessary for effective operation of fast vessels without taking ice loads into account. In the given case a conventional aluminium structure of a high speed ferry designed according to the DNV-GL HSLC code for an operation in Stockholm is investigated. For the determination of the consequences of an impact between a high speed craft and a single ice floe an analytical impact model and a series of drop tests with conical ice specimens against full-scale aluminium panels of the given vessel are presented. Plastic deformations are only observed at the stiffeners and the outer shell. The structural integrity is still given after the tests. The influence of the structural stiffness as well as the limited change in the maximum force at different energy levels during the impact is discussed.

1 INTRODUCTION

There is only scarce knowledge about ice impacts on high speed crafts. High speed crafts are designed according to the high speed craft code (HSLC code). This code enables light constructions which are necessary for an efficient operation of high speed crafts. The HSLC code considers mainly hydrodynamic loads such as slamming. Ice impacts are not included.

For a first year ice environment the Finnish Swedish Ice Class Rules (FSICR) (Transport safety agency (2010); Riska & Kämäräinen (2011)) rules are an industrial standard. But the FSICR rules are developed mainly for conventional steel structures - high speed applications and aluminium structures are not considered.

Popov *et al.* (1967) developed an energy approach which is based on a collision of two bodies for the estimation of ice forces on conventional ship structures. Daley & Liu (2010) use this approach and concluded that the methodology is not only suitable for Polar Class 7 ships but also for other ship classes.

The chosen scenario is based on a high speed ferry intended to operate as a part of the public transportation network in the Stockholm area. In Stockholm waters sea ice might pose a risk that has to be considered in the construction of the vessel. The scenario investigates a possibility during the winter that the non-ice-strengthened high speed vessel impacts an undetected free floating ice floe. A continuous operation in ice is not planned. The main dimensions of the investigated vessel are shown in Table 1.

Table 1. Main dimensions of the high speed craft

Main Dimensions		
Length	LOA	22.41 m
Length	LWL	20.68 m
Moulded breath	B	6.92 m
Moulded depth	D	3.20 m
Design draft	T	1.00 m
Displacement	Δ	48 t
Installed engine power (MCR)	P	1,400 kW
Passenger capacity		90 Passengers

The investigated test case is a single impact of an ice floe against this high speed craft build according to the HSLC code in Stockholm waters. During the investigation, the consequences and the necessity of a replacement of the affected panel should be clarified.

Therefore an analytical impact model is developed and a series of drop tests are carried out by impacting full scale aluminium hull panels with a conical ice specimen. Loads and damage levels are evaluated on the basis of the impact model and all test results.

2 TEST PANELS

The test panel is designed according to DNV-GL HSLC code (DNV GL AS (2015)). The given design loads, defined in the HSLC code, are meant to describe the hydrostatic pressure and slamming loads, using an equivalent uniformly distributed design pressure. The design pressures can be found in Table 2. The resulting aluminium test panel is presented in Figure 1.

Table 3 compares the result of the HSLC code to a corresponding structure which fulfils the FSICR 1C rules. The FSICR rules are adapted to the aluminium structure by adjusting the critical stresses. As a result, the plate thickness, following the FSICR, is three times larger and the required frame section modulus is almost thirteen times larger compared to the HSLC code. Hence a real ice class implies a higher ship mass which would reduce the efficiency of the vessel significantly.

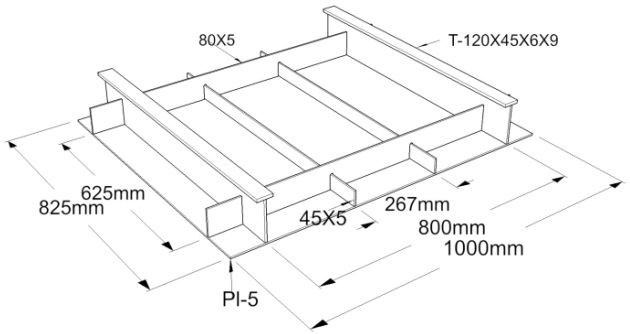

Figure 1. Tested aluminium panel according to the HSLC-code

3 DEFINITION OF THE CHOSEN IMPACT SCENARIO

The impact scenario is characterized by the impact energy of the ice floe. The impact energy determines the maximum energy entry on the ship structure. A solution of the three following physical models is necessary to compute the impact energy:

1. An ice floe model for the determination of the ice floe size,
2. a hydrodynamic model for the approximation of the impact point and direction,
3. a mechanical model for the determination of the impact energy.

Table 2. Table over the design loads according to HSLC code

Structural member	Design pressure [kPa]	Loading area [m²]	Total design load (p x A) [kN]
plate	48.1	0.167	8.02
stiffener	48.1	0.167	8.02
webframe	34.6	0.500	17.3
girder	22.8	2.000	45.68

3.1 *The ice floe model*

To develop the ice loading scenario, the ice conditions in the Stockholm area are defined using an ice growth model, because temperature measurements are available for the area while reliable ice charts are not. The used ice growth model is given by Leppäranta (1993). To determine the maximum ice thickness in the area of operation, data from ”Stockholm’s temperature series 1756-2013” is used. This dataset provides daily mean air temperatures for the Stockholm area. A generalized extreme value distribution is fitted to the maximum ice thicknesses for each winter, calculated using the ice growth model. The temperature data has a cold bias when used for prediction of current and future temperatures due to a rise in average temperatures during the last centuries. This cold bias can be handled by using the newer data, but the accuracy of the extreme value predictions decreases with the number of data points. The time period 1962-2013 is chosen, as it is the shortest time interval that provides a good fit for the extreme value distribution, resulting in a total of 50 winters. The most likely maximum ice thickness for one winter in the Stockholm area is found through the mode of the fitted Generalized Extreme Value distribution. This results in a predicted maximum ice thickness H in the Stockholm area of 0.206 m. The ice growth model is expected to provide conservative results according to Leppäranta (1993).

The loading scenario is defined as the collision between the vessel in operating condition and a floating ice floe in calm water. The ice floe is idealized as a circular disk. The ice thickness is defined as the predicted ice thickness and the diameter is defined based on the expected breaking length.

The breaking length is defined according to Lindquist (1989). This approach provides reasonable results in an ice resistance model and the floe size is therefore likely to be representative for ice floes in a broken channel. The resulting breaking length L_B of the ice floe is 1.79 m, calculated as one third of the characteristic length L_c according to Equation 1. Input values are the elasticity modulus of ice E, the ice thickness H, the Poisson number μ of ice, the density of water ρ_{W} and the standard gravity g.

$$L_{\mathrm{B}} = \frac{1}{3} L_c = \frac{1}{3} \sqrt[4]{\frac{EH^3}{12(1-\mu^2)\rho_{\mathrm{W}} g}} \qquad (1)$$

The shape of the impacting ice floe is defined as a

Table 3. Exemplary comparison of structures according to HSLC code and FSICR

	HSLC code		FSICR	
	design pres. [MPa]	dim. [mm]	design pres. [MPa]	dim. [mm]
plate	0.048	5	1.332	15.5
frame	0.048	FL45x5	1.305	FL150x11

circular disk with height 0.206 m and diameter 1.79 m according to the breaking length.

3.2 *Approximation of the impact point*

An impact model is created by calculating the floating condition of the vessel, the floating equilibrium of the ice floe, and thereby defining the impact velocity, location, and angle. The planning condition of the vessel in flat water is calculated using Savitsky's method (Savitsky (1964); Savitsky & Brown (1976)) and the floating condition of the ice floe is defined by the hydrostatic equilibrium. The impact location is determined as the foremost point of the hull, at the height of the upper corner of the ice floe, see Figure 2. The dead rise angle is not considered and the model thereby becomes two dimensional, as the keel line is used to define the impact location and the panel normal. This simplification is conservative since the inclusion of the dead rise angle will increase the angle between the direction of travel and the panel normal.

The impact velocity vector is determined from the vessel velocity, normal to the impacted panel, at the impact location.

3.3 *Impact modelling*

Popov *et al.* (1967) describes the impact of a ship and an ice floe as a 3D event, which can be reduced to an equivalent 1D problem. Based on the Popov approach Daley & Liu (2010) shows a formulation for computing the impact energy IE. The impact energy depends on the effective mass of the ice floe $M_{\mathrm{E,ice}}$ and the ship $M_{\mathrm{E,ship}}$ as well as the impact velocity V:

$$IE = \frac{1}{2}\left(\frac{1}{M_{\mathrm{E,ship}}} + \frac{1}{M_{\mathrm{E,ice}}}\right)^{-1} V^2 \qquad (2)$$

The effective masses M_E are determined by solving the six equations of motion for each body of the rigid body collision.

$$F_n = M_{\mathrm{E}}\ddot{\zeta}_n \qquad (3)$$

The effective mass is computed by the following equation:

$$M_{\mathrm{E}} = \left(\frac{l^2}{M_{\mathrm{x}}} + \frac{m^2}{M_{\mathrm{y}}} + \frac{n^2}{M_z} + \frac{\lambda^2}{I_{\mathrm{x}}} + \frac{\mu^2}{I_{\mathrm{y}}} + \frac{\nu^2}{I_{\mathrm{z}}}\right)^{-1} \qquad (4)$$

l, m and n are direction cosines of the impact point and λ, μ and ν are the level arms to the principle axis. The principle axes are fixed in the centre of gravity of each body. Hydrodynamic effects are considered by added masses for the masses M and mass moments I. For details compare Daley & Liu (2010).

The added mass of the high speed vessel is approximated by a solution of a wedge. The used solution can be found in Faltinsen (2005).

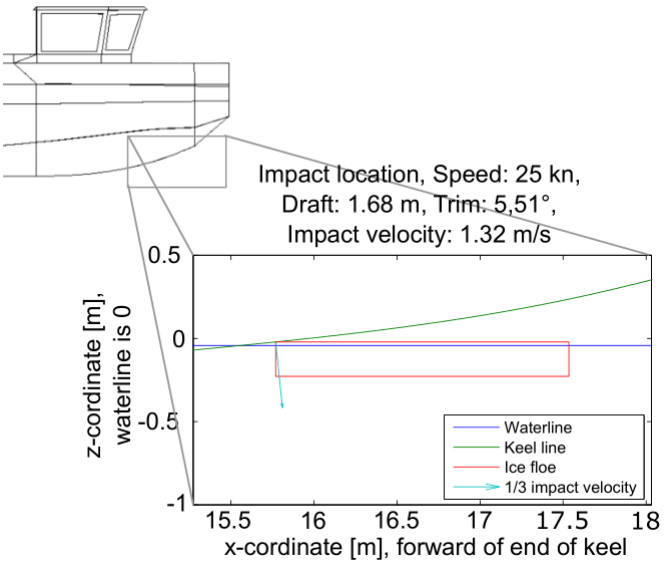

Figure 2. Illustration of the impact scenario

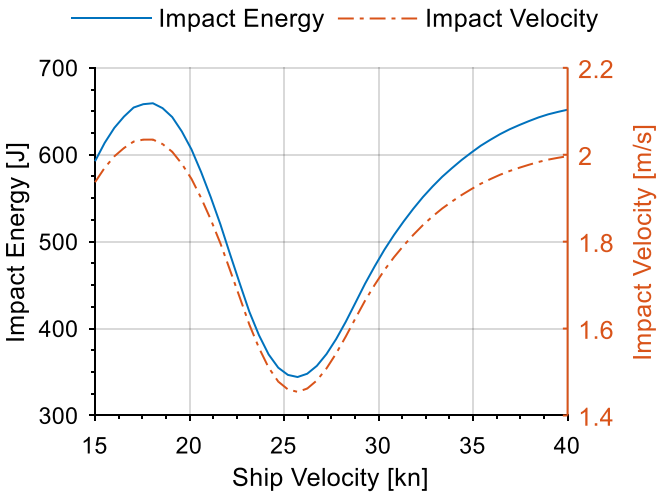

Figure 3. Impact energy results according to the impact model

The added mass of the ice floe in heave is modelled as a half-submerged circular disk according to Pedersen et al. (2010).

$$M_{\mathrm{zh}} = \frac{1}{2}\rho_W \cdot 0.64\pi\frac{4}{3}\left(\frac{L_{\mathrm{B}}}{2}\right)^3 \qquad (5)$$

The added mass in surge is modelled as a long slender cylinder, by considering 2 dimensional flows around a cylindrical cross section over the submerged height of the ice floe h (Pedersen *et al.* (2010)). This assumption is considered conservative, as the added mass should decrease when taking three dimensional effects into account.

$$M_{\mathrm{xh}} = h\rho_W\pi\left(\frac{L_{\mathrm{B}}}{2}\right)^2 \qquad (6)$$

The added inertia in pitch is modelled using strip theory. The pitch added inertia of a strip is modelled by the heave added mass of the strip and the heave acceleration due to the pitch acceleration of the strip. The result is an expression for the added moment of inertia, depending on the density of the water and the diameter of the ice floe.

$$I_h = \frac{\rho_{\mathrm{W}}\pi}{240}L_{\mathrm{B}} \qquad (7)$$

Figure 3 shows the result of the impact model according to Equation 2 for the given scenario. The result mainly follows the change of the impact velocity, which is determined by the trim and the normal to the impacted panel. A decrease of the impact velocity bases on the change of the trim and the given form of the bow. The velocity dependence on the effective mass of the vessel is significant in a range of 40% to 80% of the ship mass but not relevant because of the huge difference between the effective mass of the ship and the ice floe. However is the effective mass of the ice floe, which is nearly velocity independent, important for the impact energy. The effective mass of the ice floe amounts to approximately 0.75% of the ship mass. At a ship speed of 18 kn the impact energy raises the peak value of 660 J.

4 PRESENTATION OF TESTS

The realized tests are a series of drop tests based on the presented impact scenario. All drop tests are performed at TUHH in the mechanical laboratory of the Institute for Ship Structural Design and Analysis. The drop tests are carried out using full scale hull panels and a drop weight on rails. To approximate the real life impact between an ice floe and a high speed craft, the hammer is equipped with an ice cylinder. Impact mass and impact velocity are determined, using the calculated impact energies from the impact model. The test program contains three test series against a rigid structure and two series against the aluminium test panels.

4.1 *Test setup*

The equipment in the laboratory, used in this test series, includes a drop tower, a cold room, a band saw, and a coning machine. The drop tower is sketched in Figure 4.

The testing is carried out by placing the test panel on a set of load cells under a drop weight. The drop weight is running on a set of vertical rails to increase repeatability. The drop height determines impact velocity. The impact mass is adjustable from 220 kg to 600 kg, using steel ballast.

Ice specimens are frozen into a mount, which is bolted onto the drop weight. A release hook for a life raft is used to release the drop weight. Height stops, consisting of two wooden beams and mounted on stiff rubber blocks, are installed to protect the test rig. The height stops also ensure that the test panels will be impacted by the ice specimen only, and not by the drop weight, in case the ice specimen is completely crushed.

The following measurement equipment is used during testing. Each value is recorded with a sampling frequency of 1 kHz:

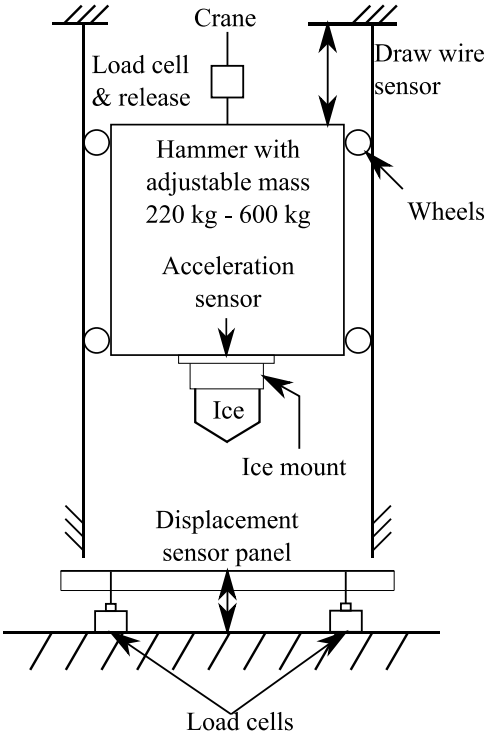

Figure 4. Illustration of the experimental setup

- A load cell in the crane for accurate measurement of the impact mass
- An accelerometer and a draw-wire displacement sensor for measurement of accelerations and velocities
- Four load cells under the plate panel for measurement of the total impact load
- A displacement sensor under the panel for measuring the dynamic deformation at the centre of the plate panel
- Pressure mapping foil sensors for measuring the pressure distribution during testing
- Strain gauges on one of the aluminium panels for measuring stresses and structural response

The pressure mapping foil is part of the TekScan system. TekScan is a grid based piezo resistive tactile pressure measurement foil (Paikowsky & Hajduk (1997)). Four 5101 load sensors, with a nominal pressure of 3000 PSI, are used to measure the total load. The sensors are covered on both sides with KAPTON® HN500 foil. The edges of the foil are glued together by tape. The foil protects the sensor against mechanical loads like cuts and shear stresses, water as well as minimizes noise in the measurements. The test frequency for the TekScan measurement is 730 Hz which is the maximum test frequency of this sensor.

4.2 *Ice Specimens*

Ice specimens are cylindrical with a diameter of 203.4 mm and a conically shaped tip. The angle of

Figure 5. Ice specimen preparation

the cone is 30°. The total length of the specimen is 350 mm. The ice specimens are frozen using commercially available crushed ice and distilled water. The added water is cooled down to 5°C before use to prevent excessive melting of the crushed ice.

The ice specimens are frozen in PVC-U pipes at -25°C in the cold room. To avoid cracks in the ice specimens they are frozen from the bottom up. This is done by adding a thin metal plate to the bottom, creating a direct connection between the metal plate and the metal floor in the cold room. This provides an excellent heat flux while the top of the specimens are covered with insulating material.

After freezing, the mould is removed under ambient conditions in the laboratory. Immediately after removal, the ice specimens are stored in the cold room. Each specimen is frozen to the mount, coned, and moved back into the cold room before testing. This process ensures consistency in the shape and material properties of the specimens. The coning is conducted by using a make-shift coning machine. The ice fitting with the ice specimen is bolted onto a turntable and a blade is used to shape the rotating ice specimen. The process is similar to a milling operation. The cone shaping process takes around 2 minutes at 300 rpm. The coning process can be seen in Figure 5.

Table 4. Test series

Test series/ Test number	PM, AM		PV, AV	
	Mass [kg]	Vel. [m/s]	Mass [kg]	Vel. [m/s]
0	224*	1.5*	224*	1.5*
1	300	1.5	224	1.77
2	400	1.5	224	2.05
3	500	1.5	224	2.29
4	600	1.5	224	2.51

*Used for the repeatability test series, PR

4.3 *Test program*

The influence of increasing mass, velocity, impact energy, and the ice-structure interaction is investigated through a test program with a total of 22 drop tests. In order to evaluate the loads and the repeatability of the tests, a series of pre-tests are conducted using a rigid plate. The initial test series is composed of three pertest series: PR (Repeatability tests), PM (Increasing mass) and PV (Increasing velocity). Two test series are conducted using aluminium test panels: AM (Increasing mass) and AV (Increasing velocity). The energy level is determined by the presented impact model. During each test series the kinetic energy at impact increases. The last test (number 4) reaches 675 J. The used impact mass varies in steps of 100 kg which is constrained by the available steel ballast. The kinetic energies at impact of the mass and velocity test series are comparable. The resulting masses and velocities are presented in Table 4.

5 TEST RESULTS

Test results include general observations on the behaviour of the system, along with measurements of forces, energies and deformations, and reflection upon the effect of the results on the high speed craft scenario.

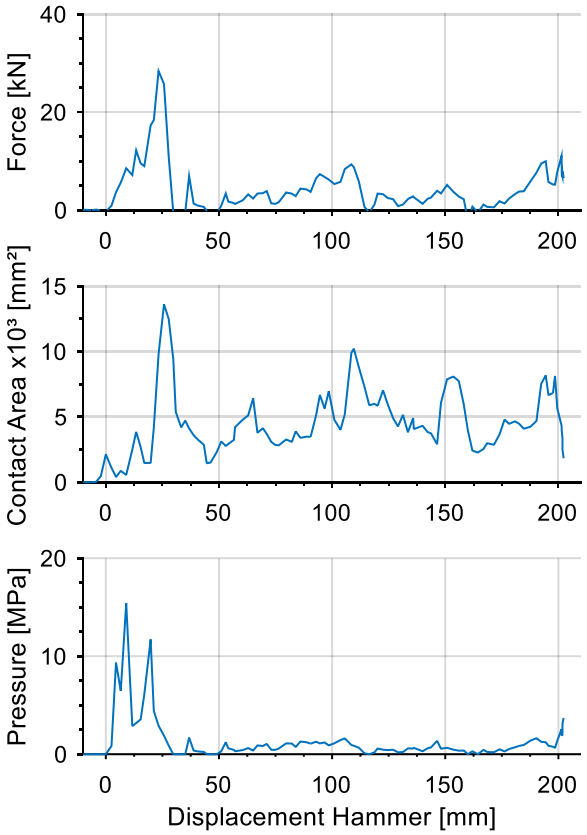

Figure 6. Test results of test AM2

5.1 *Forces and energies*

The impact force is measured by the load cells under the impacted panel. The kinetic energy at impact E_{Imp} is determined by the drop mass and the velocity, measured by the draw-wire sensor at first contact between ice and aluminium panel.

$$E_{\mathrm{Imp}} = \frac{1}{2} m V^2 \tag{8}$$

At first contact, the tip of the ice behaves in a ductile manner and builds up pressure until crushing and cracking of the ice specimen is initiated. The peak load seems to occur just before initiation of large cracks in the ice specimen. Afterwards, the force drops dramatically and a fluctuating load is caused by spalling. This behaviour can be seen in Figure 6, where the area is taken from TekScan measurement. The presented pressure is the average contact pressure.

For the pre-test series with a rigid plate the peak loads occurs in a range from 13 mm to 20 mm displacement, after first contact. This value changes between 22 mm and 35 mm for the flexible structures, due to the elastic and plastic deformation of the panel. The two initial tests on the aluminium plate panels, AM0 and AV0, show a different behaviour than all of the other tests. The ice specimens are bouncing on the panel and no big spalls break off the specimens. A maximum contact pressure of 25 MPa is calculated for test AV0. This phenomenon is attributed to the flexibility of the aluminium panels and can be seen in Figure 7.

The maximum forces of all tests are shown in Figure 8. The tests are plotted against the kinetic energy at impact. The maximum forces are only evaluated in the first 150 mm displacement after first contact. This is done to prevent the mount having an effect on the results, as it could increase the load from the ice due to the ice being confined (change in boundary conditions). The maximum forces for the tests are between 12.94 kN and 34.96 kN. The maximum force for most tests with a kinetic energy of 352 J is between 20 kN and 25 kN. Only one outlier with a maximum force of 32.66 kN is observed. The behaviour indicates a sufficient reproducibility for all test series.

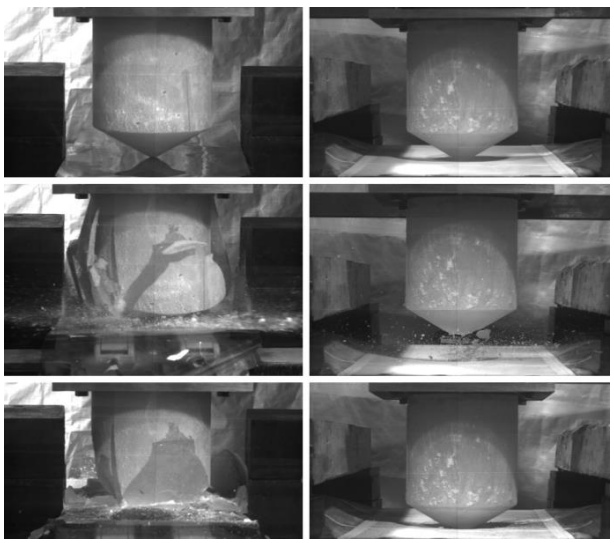

Figure 7. Compression of tests PR0 (left) and AV0 (right)

There is no clear trend between the maximum forces and the kinetic energy at impact. For the test series against a rigid plate (PM and PV), the maximum force decreases slightly with increasing kinetic energy, but this trend is not seen in the test against the aluminium panels (AM and AV). The variation of the maximum force of the test series AM and AV is significantly higher than for tests against a rigid plate. It is concluded that the stiffness of the impacted structure has a significant influence on the magnitude of the load, but no clear trends in the influence of velocity and mass are found.

In Figure 9 is the collision energy as a function of kinetic energy at impact presented. The collision energy E_{Col} is calculated by the force from the load cells under the panel, integrated over the displacement, measured by the draw wire sensor during the impact. The collision energy is higher than the kinetic energy because of the potential energy left in

$$E_{\mathrm{Col}} = \int F \, ds \tag{9}$$

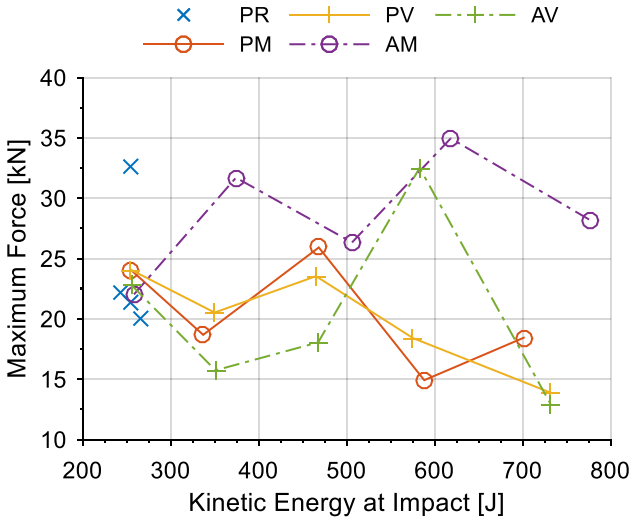

Figure 8. Maximum forces of all tests until 150 mm displacement

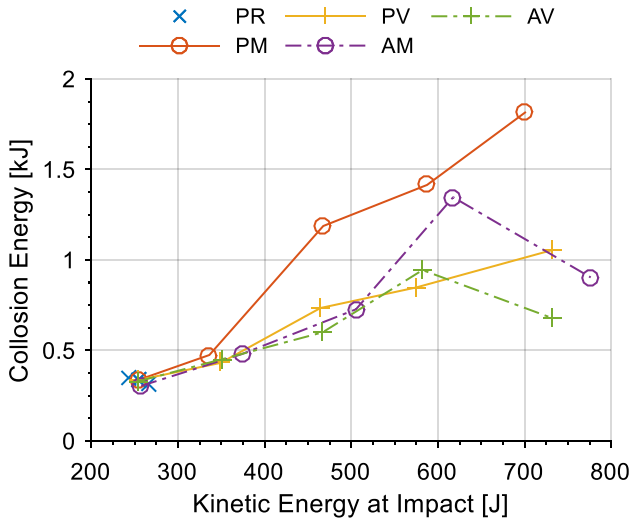

Figure 9. Collision Energy of all tests

the crushing length after the first contact.

The collision energy is generally increasing with the kinetic energy in the impact. All test series achieve higher collision energies than 660 J, which is the maximum impact energy of the impact model for the given scenario.

5.2 *Measured deformations*

Deformations are measured with a laser measurement system along each of the smaller stiffeners (position a and c) and parallel to the stiffeners at the centre-line of the plate panel (position b). Figure 10 shows the deformation of the panel before the tests (AMb) and after each test (AM0-AM4). The missing data points in Figure 10 a) and c) at x≈-300 mm and x≈300 mm are caused by installed strain gauges making the laser displacement measurements invalid.

After the first impact (AM0), the panel is indented by 7 mm at the centre and approximately 1 mm at the middle of the stiffeners. The deformation behaviour can be described as rather local.

In the following tests, the deformation shifts from a primarily local to a primarily global behaviour. This is illustrated using the displacement increase at the middle of the stiffeners and the displacement increase at the plate centre as a reference.

The second test causes a deformation increase of around 3 mm at plate centre and 1.7 mm at the stiffeners. This represents a ratio of 1.76 in contrast to 7 from the first test. There is no additional deformation observable in the third test, which can be explained by the slightly lower maximum load (see Figure 8). A slight additional deformation increase, approximately 1 mm, is seen after test four, with an absolute deformation of 12.3 mm at the plate centre and 4 mm at the middle of the stiffeners. The ratio for the displacement increase is 1. The maximum load of the final impact is significantly lower, for which reason no further deformations are observed. The maximum deformation after all tests is 12.3 mm in the centre of the panel.

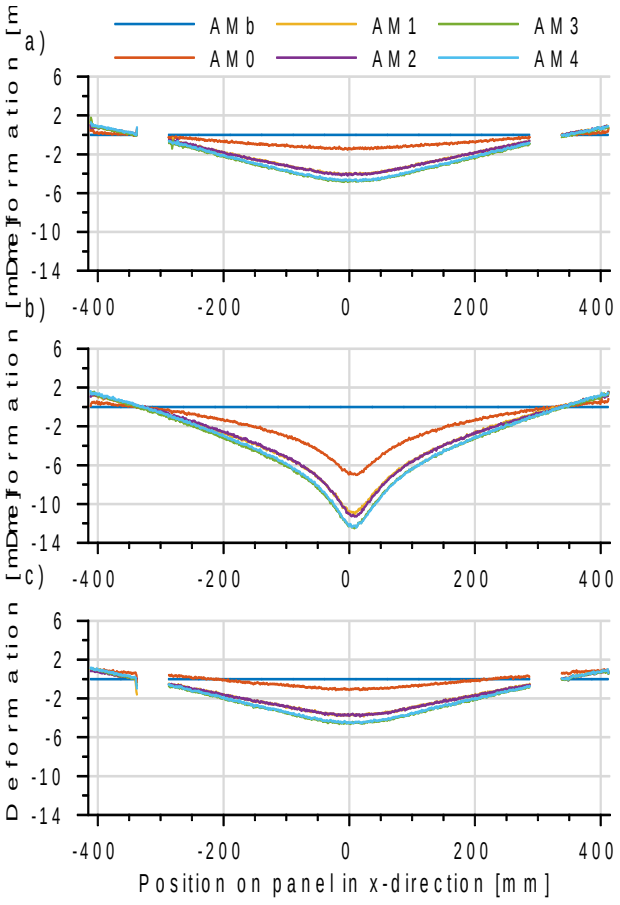

Figure 10. Deformation states of test series AM at positions a), b) and c)

Table 5. Load comparison

Structural member	Total design load	Maximum test loading AV	Maximum test loading AM
Plate	8.02 kN	32.55 kN	34.94 kN
Stiffener	8.02 kN	16.27 kN	17.47 kN
Webframe	17.31 kN	16.27 kN	17.47 kN
Girder	45.68 kN	16.27 kN	17.47 kN

5.3 *Damage levels and consequences for the vessel*

The design loads for the plate panel according to HSLC code is a uniformly distributed design pressure, while the applied load is highly localized. The presented loads in Table **5** are therefore not directly comparable, but the total load can be compared. The total design load for each structural member is calculated as the uniformly distributed pressure times the design area for the structural member. The maximum test loading for the plate field is defined as the measured maximum load during testing. There is one stiffener on each side of the loaded area. Therefore the total load for one stiffener is taken as half of the measured maximum load.

No measurable deformations were observed on the webframes and the girders, where the load is in the order of or smaller than the total design load. Taking safety factors into account there is a small deformation of the stiffeners which corresponds well to the maximum load being roughly twice the total design load. There is a significant, but not critical, deformation of 13 mm at the centre of the plate field, which corresponds well to the maximum load being more than four times higher than the total design load.

The structural integrity of the aluminium test panel is intact after testing. The damage is limited to local deformations in smaller structural members and plating. Dents up to three times plate thickness are acceptable for operation by a common maritime practice. Thus a 13 mm deep dent is noncritical for a 5 mm thick plate. This shows that a HSLC vessel, which is not designed for ice impact, seems to be able to tolerate an individual accidental impact with

a free floating ice floe without requiring immediate repairs.

6 CONCLUSION

A scenario based model for investigating the impact between an ice floe and a high speed craft is presented. The impact of an ice floe on a high speed craft in operation was defined, taking added mass and impact geometry into account.

A series of drop tests have been carried out, using input from the impact model and full size plate panels designed according to the HSLC code on the basis of the vessel in the defined scenario. These drop tests have provided insight into the behaviour of the load. All drop test series achieve higher collision energies than 660 J which is the maximum impact energy of the analytical impact model for the presented scenario of an individual accidental impact between a free floating ice floe and a high speed craft. Nevertheless, the structural integrity of the test panels is still given after the test series.

The investigation of the ice loading demonstrated that the load is highly influenced by the stiffness of the impacted structure. The amount of energy that can be transferred in a collision with an unconstrained piece of ice is found to be limited by the failure mechanisms of the ice. No clear relation between the kinetic impact energy and the maximum force was observed. It is concluded that the maximum force is more dependent on other factors, for example the material properties of the ice and the stiffness of the impacted structure.

Based on the findings in this article it is concluded that single ice impacts on a high speed craft under light ice conditions would result in slight but non-critical damages.

ACKNOWLEDGEMENTS

TUHH acknowledges the financial support of the German Research Foundation and Lloyd's Register Foundation. Lloyd's Register Foundation supports the advancement of engineering-related education, and funds research and development that enhances safety of life at sea, on land and in the air.

REFERENCES

Daley, C. & Liu, J. 2010. Assessment of Ship Ice Loads in Pack Ice. *ICETECH*.

High speed and light craft code. 2015, *DNV GL AS*.

Faltinsen, O.M. 2005. Hydrodynamics of high-speed marine vehicles. Cambridge Univ. Press, Cambridge.

Leppäranta, M. 1993. A Review of Analytical Models of Sea-Ice Growth, *University of Helsinki*, Helsinki.

Lindquist, G. 1989. A Straightforward Method for Calculation of Ice Resistance of Ships. *POAC:* 722–735.

Paikowsky, S.G. & Hajduk, E.L. 1997. Calibration and Use of Grid-Based Tactile Pressure Sensors in Granular Material. *Geotechnical Testing Journal vol.* 2: 218–241.

Pedersen, P.T., Andersen, P. & Aage, C. 2010. Grundlagende skibs- og offshoreteknik, *Technical university of Denmark*.

Popov, Faddeyev, Kheysin & Yakovlev. 1967. STRENGTH OF SHIPS SAILING IN ICE: TECHNICAL TRANSLATION, Leningrad.

Riska, K. & Kämäräinen, J. 2011. A review of ice loading and the evolution of the Finnish-Swedish ice class rules. *SNAME*.

Savitsky, D. 1964. Hydrodynamic Design of planning Hulls. *Marine Technology vol.* 1: 71–95.

Savitsky, D. & Brown, W. 1976. Procedures for hydrodynamic Evaluation of planning Hulls in smooth and rough water. *Marine Technology vol.* 13: 381–400.

Transport safety agency. 2010. Finnish-Swedish ice class rules.